Hindawi
Oxidative Medicine and Cellular Longevity
Volume 2020, Article ID 9250512, 13 pages
https://doi.org/10.1155/2020/9250512

Research Article

Dexmedetomidine Postconditioning Alleviates Hypoxia/Reoxygenation Injury in Senescent Myocardial Cells by Regulating lncRNA H19 and m^{6}A Modification

Xuan Zhang,[1,2] **Qiang Fu**,[1] **Longhe Xu**,[1] **Yitian Yang**,[1] **Weixing Zhao**,[1] **Yunliang Zhang**,[1] **Hao Li**,[1] **and Weidong Mi**[1]

[1]*Anesthesia and Operation Centre, Chinese PLA General Hospital, Beijing 100853, China*
[2]*Department of Anesthesiology, Tianjin Medical University Cancer Institute and Hospital, Tianjin 300060, China*

Correspondence should be addressed to Hao Li; lihao301@126.com and Weidong Mi; wwdd1962@aliyun.com

Received 1 July 2019; Revised 21 November 2019; Accepted 20 December 2019; Published 7 January 2020

Academic Editor: Daniele Vergara

H19, a long noncoding RNA (lncRNA), reportedly protects myocardial cells (H9c2 cell line) against hypoxia-reoxygenation- (H/R-) induced injury. Dexmedetomidine (Dex) has an important myocardial protective effect, although its function and mechanism in cardiac ischemia/reperfusion (I/R) injury, especially for senile patients, requires further study. RNA N6-methyladenosine (m^{6}A) is the most abundant endogenous RNA modification. However, the effect of Dex postconditioning on RNA m^{6}A modification has rarely been reported. The aim of this study was to evaluate roles of H19 and m^{6}A modification in Dex postconditioning of aged cardiomyocytes. Hydrogen peroxide (H_2O_2) was used to induce senescence of H9c2 cells. After 6 h of hypoxia, H9c2 cells were exposed to different concentrations of dexmedetomidine (0, 500 nM, 1 μM, and 2 μM) for 6 h. After knockdown or overexpression of H19 and its downstream gene miR-29b-3p and cellular inhibitor of apoptosis protein 1 (cIAP1), Dex postconditioning experiments were performed to examine effects on myocardial cell injury. Global m^{6}A levels after H/R with or without Dex postconditioning were measured with a colorimetric m^{6}A RNA Methylation Quantification Kit. The mechanism by which RNA m^{6}A methylation regulated genes mediating H19 expression was verified by m^{6}A RNA immunoprecipitation (MeRIP), and the function of Dex postconditioning of aged cardiomyocytes was investigated. Dex postconditioning protected against H/R-induced injury of aged myocardial cells through H19/miR-29b-3p/cIAP1, increased methylation of RNA m^{6}A elicited by H/R, and attenuated H/R-induced injury by suppressing expression of the RNA m^{6}A demethylase gene alkB homolog 5 (ALKBH5). In addition, AKLBH5 regulated the expression of H19, and Dex postconditioning attenuated H/R-induced injury via ALKBH5 in aged cardiomyocytes.

1. Introduction

With the acceleration of global population aging, the morbidity of myocardial infarction (MI) is increasing. Ischemia preconditioning or postconditioning could effectively minimize ischemia/reperfusion (I/R) injury [1]. Perioperative trauma, stress, and anesthesia increase the risk for I/R injury, especially in elderly patients, whose systemic physiological function is decreased, tolerance to surgery and anesthesia are reduced, and cardiovascular adverse events are incremental [2]. Dexmedetomidine (Dex), a highly selective α2-adrenergic receptor agonist, protects organs from I/R injury by several mechanisms [3–6]. As such, it is widely used as anesthesia for cardiovascular surgery; indeed, perioperative Dex reportedly reduces the mortality rate at 1 year after surgery, as well as the incidence of postoperative complications and delirium following cardiac surgery [7]. In animal experiments, ischemic postconditioning with Dex reduced the infarct area of adult rat hearts and expression of lactate dehydrogenase, creatine kinase isoenzymes, and malondialdehyde

[8]. Although a number of new cardioprotective therapies have been discovered in the research laboratory, only a few of these have been demonstrated to improve clinical outcomes [9]. Therefore, the effect and mechanism of Dex hypoxic postconditioning on senescent cardiomyocytes still needs elucidation.

Long noncoding RNA (lncRNA), a diverse class of nonprotein-coding transcripts longer than 200 nucleotides, plays an important role in gene expression through epigenetic, transcriptional, and posttranscriptional effects. In particular, lncRNA can act as competitive endogenous RNA (ceRNA) to regulate microRNA expression [10]. lncRNA H19, a 2.3 kb noncoding RNA, reportedly has contradictory functions in cancer and, interestingly, ischemic disease [11–14]. H19 expression was upregulated by cerebral I/R as well as cellular oxygen–glucose deprivation/reperfusion, while H19 upregulation increased hypoxia-induced injury in H9c2 cells (i.e., rat myoblasts) [15, 16]. Our previous research identified hypoxic postconditioning as a potentially effective method to alleviate hypoxia-reoxygenation (H/R) injury, although it may not be effective in the aged heart. Hypoxic postconditioning failed to elicit a protective effect in senescent cardiomyocytes, which was associated with low expression of H19. H19 was found to downregulate miR-29b-3p and partially regulate cellular inhibitor of apoptosis protein 1 (cIAP1), the inhibitor of apoptosis family members. The binding sites were verified by luciferase reporter gene assays. Indeed, the H19/miR-29b-3p/cIAP1 axis was revealed to play an important role in aged cardiomyocyte apoptosis [17]. However, whether Dex postconditioning can attenuate I/R injury by regulating H19 remains to be investigated. Moreover, the mechanism by which H19 expression is regulated is unknown.

RNA N6-methyladenosine (m^6A) is the most abundant endogenous RNA modification in eukaryon. Modification of m^6A is catalyzed by a methyltransferase complex that includes methyltransferase like 3 (METTL3), methyltransferase like 14 (METTL14), and Wilms tumor 1-associated protein (WTAP) and removed by alkB homolog 5 (ALKBH5) and fat mass and obesity-associated protein (FTO). The m^6A-binding proteins such as YTH domain family proteins and heterogeneous nuclear ribonucleoprotein C (HNRNPC) execute different functions involved in RNA metabolism [18]. Several studies have reported alterations of m^6A levels upon exposure to hypoxia that could regulate lncRNA expression [19]. Therefore, the aim of this study was to determine the effect of Dex postconditioning on lncRNA H19 and RNA m^6A modification in senescent cardiomyocytes.

2. Methods

2.1. Cell Culture and Treatment. H9c2 cells were purchased from Shanghai Institute of Cell Biology (China) and cultured in Dulbecco's Modified Eagle's Medium (DMEM; Gibco, Gaithersburg, MD, USA) supplemented with 10% fetal bovine serum (FBS), 100 U mL^{-1} penicillin G, and 100 μg mL^{-1} streptomycin, at 37°C with 5% CO_2.

To stimulate H/R injury, the medium was changed to Hank's Balanced Salt Solution (HBSS; Gibco) and cells were cultured at 37°C in a hypoxic incubator (Billups-Rothenberg, San Diego, CA) filled with premixed gas (5% CO_2 and 95% N_2) for 6 h. Following 6 h reoxygenation, cells were transferred to normal culture medium and kept in an incubator at 37°C with 5% CO_2. After 6 h hypoxia, Dex postconditioning was performed with different concentrations for 6 h reoxygenation.

Various concentrations of hydrogen peroxide (H_2O_2) were added into DMEM for 4 h to induce the senescence of H9c2 cells. Subsequently, cells were transferred to normal culture medium for 24 h.

Experiment groupings and procedures for inducing senescence and H/R are shown in the Supplemental Materials (Fig. S1).

2.2. Senescence-Associated β-Galactosidase (SA-β-gal) Assay. SA-β-gal staining was performed using a SA-β-gal staining kit (Beyotime, Shanghai, China) according to the manufacturer's instructions. Briefly, cells were washed in phosphate-buffered saline (PBS, Gibco), fixed with fixative solution for 15 min at room temperature, rinsed three times with PBS, and subsequently incubated overnight at 37°C with the staining solution mix. Percentages of senescent (SA-β-gal-positive) cells were calculated in five randomly chosen fields of view for each sample. The assay was repeated in triplicate.

2.3. Apoptosis Assay. Cell apoptosis was observed by flow cytometry following propidium iodide (PI) and fluorescein isothiocyanate- (FITC-) conjugated Annexin V staining (Beyotime). Briefly, cells were suspended in binding buffer and stained with PI and FITC-Annexin V according to the manufacturer's instructions. Samples were analyzed by flow cytometry (Beckman Coulter, Brea, CA, USA).

2.4. Reactive Oxygen Species (ROS) Detection by Fluorescence Microscopy and Flow Cytometry. After treatment of cells, ROS levels were measured with a Reactive Oxygen Species Assay Kit (Beyotime) according to the manufacturer's instructions. The culture medium was changed to serum-free medium containing DCFH-DA probe for 20 min in a chamber at 37°C. After washing with serum-free medium three times, fluorescence microscopy (Nikon, Tokyo, Japan) was used to examine fluorescence. In addition, mean DCFH-DA fluorescence was quantitatively analyzed by flow cytometry.

2.5. Mitochondrial Membrane Potential Assay. Briefly, after treatment, all samples were harvested with JC-1 probe (Beyotime) at 37°C for 20 min. Next, stained cells were washed twice with precooled dye buffer. Fluorescence microscopy was used to observe the fluorescence, while ratios of green/red cells were quantitatively analyzed by flow cytometry.

2.6. Cell Transfection. siRNAs against rat H19, cIAP1, and ALKBH5, as well as rno-miR-29b-3p mimics, rno-miR-29b-3p inhibitor, and their negative controls (NC), were purchased from GenePharma (Shanghai, China). The previously

confirmed siRNA sequences used in the study are shown in the Supplemental Materials (Table S1). Pairs of siRNAs were mixed for transfection into cells. H19 siRNA mix, cIAP1 siRNA mix, ALKBH5 siRNA mix, rno-miR-29b-3p mimics, rno-miR-29b-3p inhibitor, and their negative controls (100 nM) were combined with Lipofectamine RNAiMAX (Invitrogen, Carlsbad, CA, USA) according to the manufacturer's instructions. After 48 h, samples were used in the following experiments.

Full-length sequences of H19 and the CDS region of ALKBH5 were cloned into pcDNA3.1. Lipofectamine 2000 reagent (Invitrogen) was used for cell transfection according to the manufacturer's instructions.

2.7. Cell Viability Assessment. Cell viability was determined using a Cell Counting Kit 8 (CCK-8) assay (Dojindo, Kumamoto, Japan). Cells were seeded in 96-well tissue culture plates at a density of 2×10^4 mL^{-1}. After treatment, cells were cultured in DMEM with 10% CCK-8 for 1 h, and then numbers of cells were determined by measuring optical absorbance at 450 nm. The assay was repeated in triplicate.

2.8. Quantitative Real-Time Polymerase Chain Reaction (qRT-PCR). qRT-PCR was carried out on a CFX96 TM Real-Time System instrument (Bio-Rad, Hercules, CA, USA). Total RNA was extracted using TRIzol (Invitrogen). RNA was reverse-transcribed with a reverse transcriptase kit (Takara, Kusatsu, Japan) and subjected to qRT-PCR using SYBR Green (Takara) according to the manufacturer's instructions. Primers for qRT-PCR are listed in the Supplementary Materials (Table S1). GAPDH was used as an endogenous control.

miRNA was converted into cDNA using a miRcute Plus miRNA First-Strand cDNA Synthesis Kit (TIANGEN, Beijing, China) and was quantified with a miRcute miRNA qPCR Detection Kit (TIANGEN). U6 was used as a reference gene.

Each sample was run in triplicate. Data were analyzed according to the $2^{-\Delta\Delta Ct}$ method.

2.9. Immunoblotting. Cells were rinsed twice with PBS and then lysed for 30 min on ice in lysis buffer. Proteins were quantified using a BCA Protein Assay Kit (Beyotime). After separation using sodium dodecyl sulfate–polyacrylamide gel electrophoresis, proteins in gels were transferred onto polyvinylidene difluoride membranes, which were then blocked with nonfat milk for 1 h at room temperature. Membranes were then incubated overnight with primary antibody at 4°C, followed by washing and incubation with an appropriate horseradish peroxidase-conjugated secondary antibody for 1 h at room temperature. Signals were detected using a chemiluminescence imaging system (Bio-Rad). Blots were probed using antibodies against Bcl-2, Bax, cIAP1, ALKBH5 (Proteintech, Wuhan, China), p53 (Cell Signaling Technology, Danvers, MA, USA), and GAPDH (Santa Cruz Biotechnology, Dallas, TX, USA) as a loading control.

2.10. m^{6}A Quantification. Changes in global m^{6}A levels of mRNA were measured using an m^{6}A RNA Methylation Quantification Kit (Colorimetric; Abcam, Cambridge, UK) according to the manufacturer's protocol. For analysis of each sample, 200 ng of RNA was coated on an assay well and then the capture antibody solution and detection antibody solution were added individually at suitably diluted concentrations. m^{6}A levels were quantified colorimetrically by reading the absorbance at a wavelength of 450 nm; calculations were performed based on a standard curve.

2.11. RNA Immunoprecipitation. RNA immunoprecipitation (RIP) experiments were performed using Magna RIP RNA-Binding Protein Immunoprecipitation Kit (Millipore Corporation, Burlington, MA, USA) according to the manufacturer's protocol and previous research [20]. Antibodies against m^{6}A (SYSY, Goettingen, Germany) or IgG were diluted to 1 : 50, previously bound to magnetic beads. Control and ALKBH5 knockdown H9c2 cells were lysed in RIP lysis buffer. Samples of each lysate were aliquoted to serve as input controls, while the remaining lysates were immunoprecipitated with precipitation magnetic beads. Beads and input were then treated with proteinase K buffer solution for 0.5 h at 55°C. Subsequently, RNAs were isolated and purified by phenol:chloroform:isoamyl alcohol extraction from inputs and precipitation magnetic beads. Coprecipitated RNAs were detected by qRT-PCR.

2.12. Statistical Analysis. All statistical analyses were performed using SPSS 18.0. Measurement data are expressed as mean ± standard deviation (SD). Differences between two groups with normally distributed data were evaluated using Student's *t*-test. Comparisons of more than two groups were performed using one-way analysis of variance followed by Tukey's multiple comparisons test. $P < 0.05$ was considered statistically significant.

3. Results

3.1. H_2O_2 Induced Senescence of the Myocardial Cell Line H9c2. H9c2 cells were cultured in DMEM containing different concentrations of H_2O_2 (0, 75 μM, 150 μM, 300 μM, or 600 μM), for 4 h before replacement with normal culture medium. After 24 h, SA-β-gal staining was used to evaluate ratios of aged cells. Compared with the control group, proportions of cells stained by β-gal increased with increasing concentrations of H_2O_2. However, exposure to 300 μM or 600 μM H_2O_2 resulted in shrinkage, reduced size, and obvious rounding of cells (Figure 1(a)). Cell viability also declined with increasing concentrations of H_2O_2 (Figure 1(b)). When the concentration of H_2O_2 was higher than 150 μM, expression of senescence-associated proteins p21 and p53 was remarkably elevated (Figure 1(c)).

According to data described above, a final concentration of H_2O_2, 150 μM H_2O_2 was selected as the final concentration to establish the senescence model for 4 h intervention, and subsequent experiments were conducted 24 h later. At this concentration and time, the proportion of senescent cells was increased, but the state of cells was relatively better, thus allowing them to withstand subsequent hypoxia and transfection experiments.

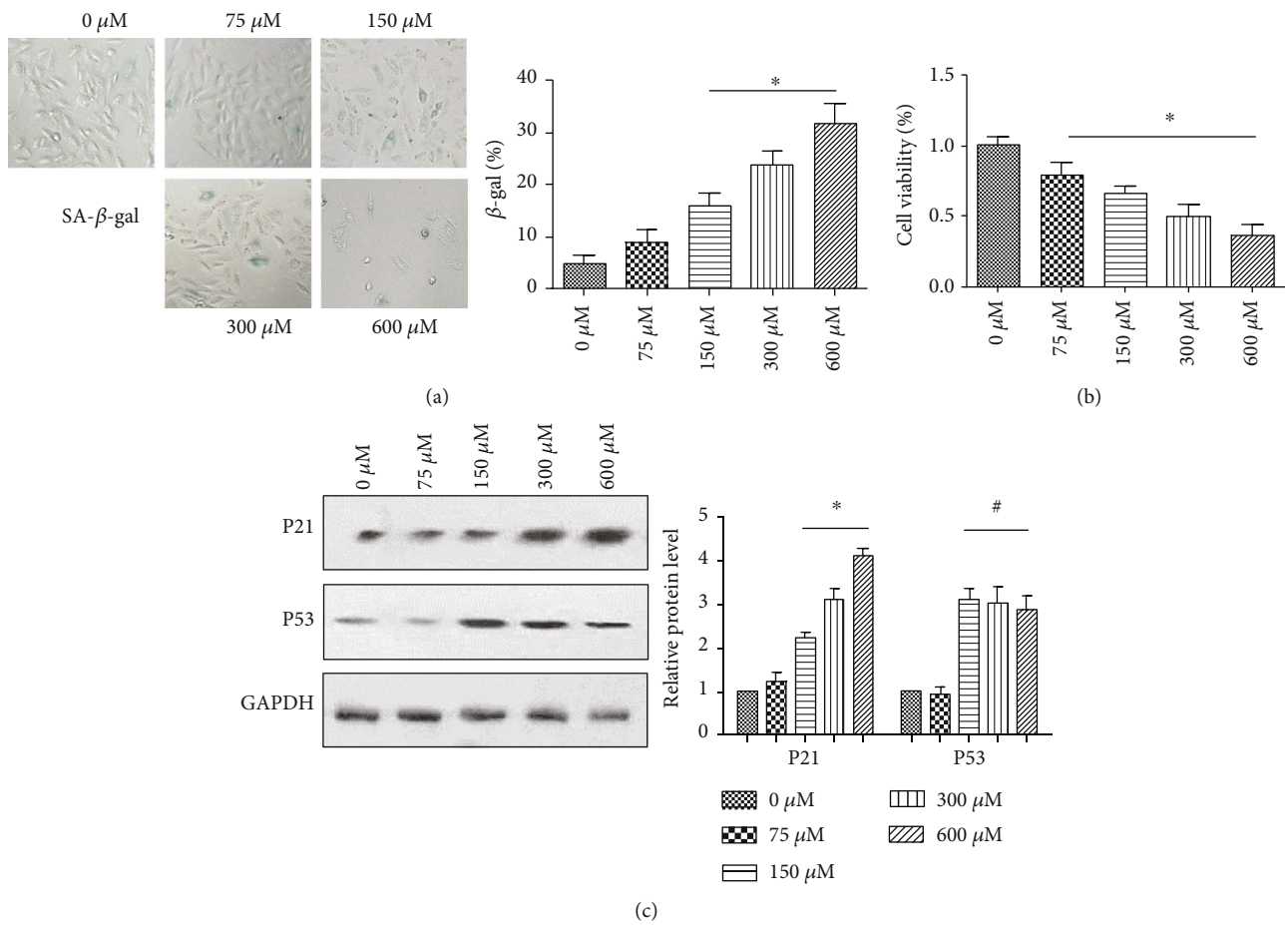

Figure 1: H_2O_2 induced senescence of the myocardial cell line H9c2. (a) After 4 h exposure of H9c2 cells with the final concentrations of 0 μM, 75 μM, 150 μM, 300 μM, or 600 μM H_2O_2, medium was replaced with normal DMEM for 24 h. Cells were then stained with SA-β-gal, and proportions of blue cells were calculated (mean ± SD, $n = 3$; $F = 49.98$, $P < 0.05$, $*P < 0.05$ vs. 0 μM). (b) A CCK-8 assay was used to detect the viability of each treatment group (mean ± SD, $n = 3$; $F = 30.32$, $P < 0.0001$, $*P < 0.05$ vs. 0 μM). (c) Expression of senescence-associated proteins P21 and P53 in each group was detected by western blot (mean ± SD, $n = 3$; $*P < 0.05$, $^{\#}P < 0.05$ vs. 0 μM).

3.2. Dex Hypoxic Postconditioning Attenuated Oxidative Stress Damage and H/R-Induced Apoptosis of Senescent Cardiomyocytes. After H9c2 cells were cultured for 4 h with 150 μM H_2O_2, H/R and Dex hypoxic postconditioning were performed 24 h later. The medium was changed to HBSS, and cells were kept in an incubator for 6 h hypoxia. The H/R and control groups were replaced with DMEM containing 10% FBS, and Dex postconditioning groups were treated with different concentrations (500 nM, 1 μM, and 2 μM) of Dex for 6 h. The ROS probe DCFH-DA was used to detect the oxidative stress level of each group, and relative quantitative analysis of mean fluorescence intensity was conducted by flow cytometry. The results indicated significantly increased ROS levels after H/R and decreased ROS levels in the cytoplasm after 1 μM or 2 μM Dex treatment (Figure 2(a)). Mitochondrial membrane potential was detected by JC-1 probe. Ratios of green/red fluorescence intensity increased after H/R but were significantly reduced by 1 μM Dex (Figure 2(b)). Ratios of apoptotic cells were analyzed by flow cytometry using Annexin V-FITC/PI staining. With Dex postconditioning at concentrations of 1 μM or 2 μM, the proportion of apoptotic cells was decreased (Figure 2(c)). Compared with the H/R group, cell viability was increased by 1 μM Dex postconditioning (Figure 2(d)). mRNA expression levels of PUMA after 1 μM Dex postconditioning were lower than those observed in the H/R group (Figure 2(e)). Moreover, ratios of Bcl-2/Bax protein expression in the H/R +1 μM Dex and H/R+2 μM Dex groups were increased (Figure 2(f)). Thus, 1 μM Dex postconditioning after 6 h hypoxia had a protective effect against H/R injury in H9c2 cells.

3.3. Dex Postconditioning Alleviated H/R-Induced Injury by Upregulating H19. To explore the relationship between Dex and H19, we first detected the expression of H19 following H/R and Dex postconditioning. Cells were divided into five groups, treated with H_2O_2 for 4 h, and then transferred to normal medium for 24 h. Next, H/R and Dex hypoxic postconditioning were performed. After H/R, H19 expression was decreased compared with the normal group, while its expression was increased in the 1 μM and 2 μM Dex groups after 6 h postconditioning (Figure 3(a)). When transfected with siH19, H19 expression in aged H9c2 was further decreased but was still increased following 1 μM Dex postconditioning for 6 h (Figure 3(b)). Cells were transfected with

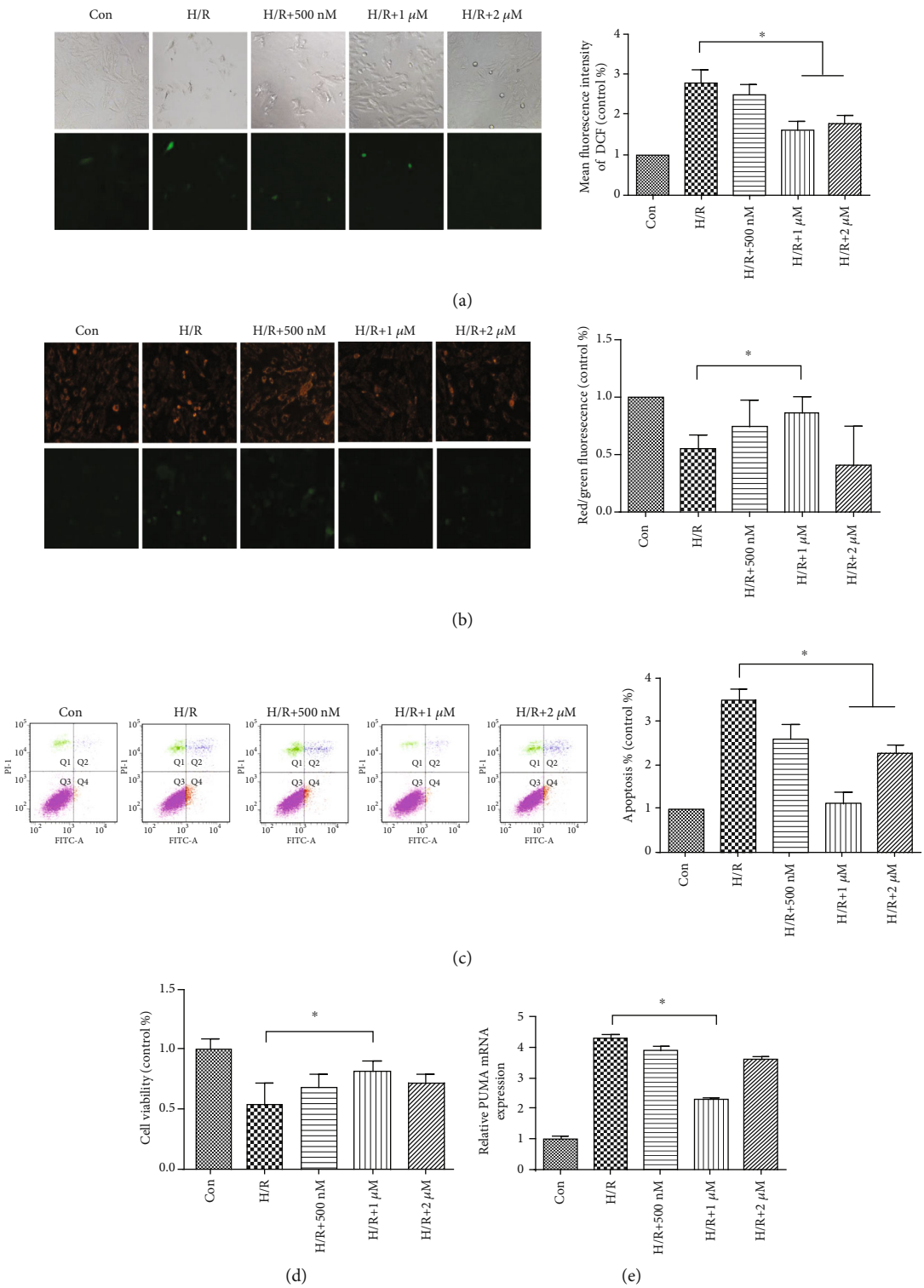

Figure 2: Continued.

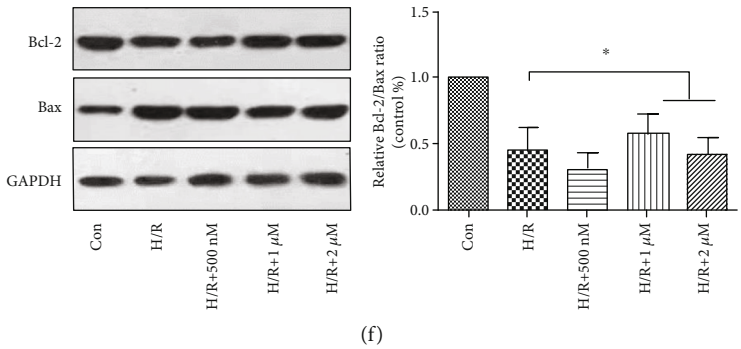

Figure 2: Dexmedetomidine (Dex) hypoxia postconditioning attenuated oxidative stress damage and hypoxia/reoxygenation-induced apoptosis in senescent cardiomyocytes. (a) Senescent cardiomyocytes were exposed to 0, 500 nM, 1 μM, or 2 μM Dex for 6 h after hypoxia for 6 h. Cells were stained by DCFH-DA to measure levels of reactive oxygen species. Mean fluorescence intensity of DCF was detected by flow cytometry. (b) A JC-1 probe was used to observe and detect fluorescence ratios of red and green in each group. (c) FITC/PI staining was used to detect ratios of apoptotic cells in each group by flow cytometry. (d) Viability of senescent H9c2 cells treated with different concentrations of Dex postconditioning was measured by CCK-8. (e) Expression of PUMA mRNA in each group was detected by RT-PCR. (f) Ratios of Bcl-2/Bax were evaluated by western blots. Mean ± SD, $n = 3$; $*P < 0.05$ vs. the H/R group.

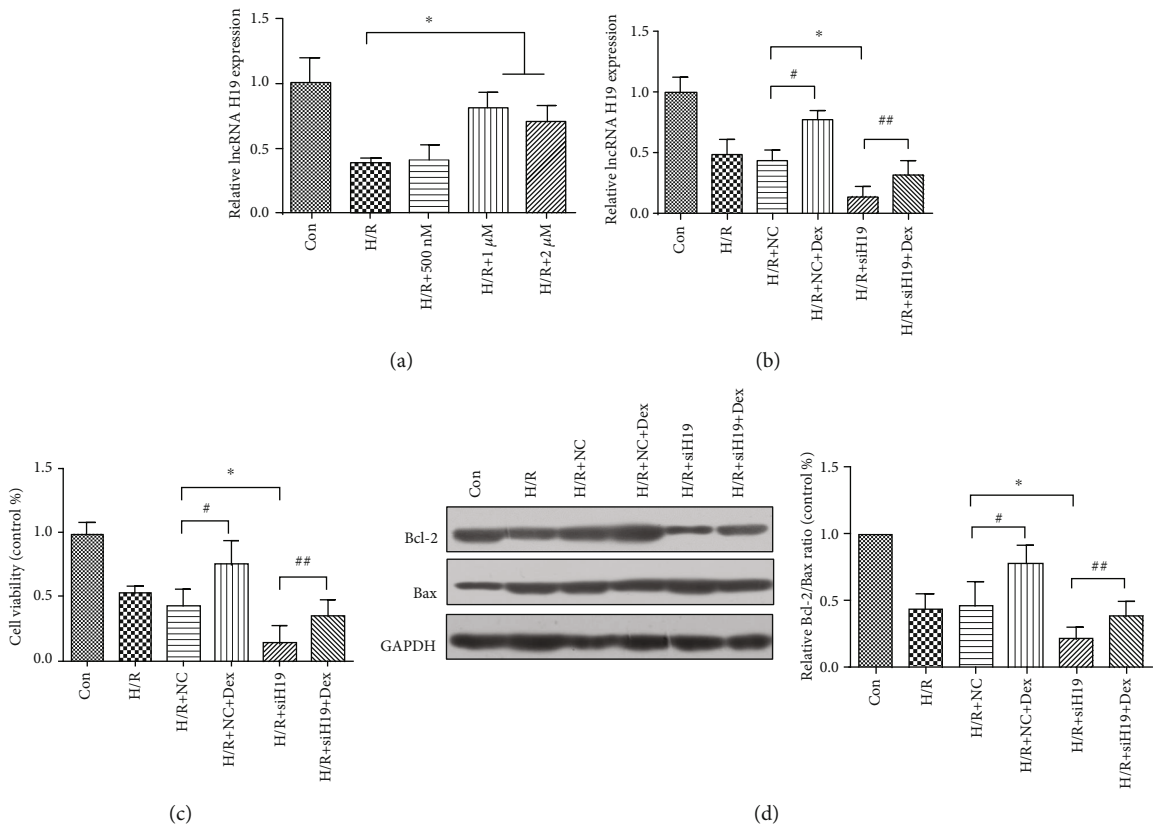

Figure 3: Dexmedetomidine (Dex) postconditioning alleviated hypoxia/reoxygenation injury by upregulating H19. (a) H19 expression after exposure to different concentrations of Dex and hypoxia postconditioning was detected by RT-PCR (mean ± SD, $n = 3$; $*P < 0.05$ vs. the H/R group). (b) After 24 h, normal DMEM culture was replaced with 150 μM H_2O_2 for 4 h, and H9c2 cells were transfected with siH19 or a negative control (NC) siRNA. After hypoxia for 6 h, 1 μM Dex was added during reoxygenation for 6 h. Expression of H19 was detected by RT-PCR. (c) Cell viability was evaluated using a CCK-8 assay. (d) Ratios of Bcl-2/Bax protein expression were measured by western blotting. Mean ± SD, $n = 3$; $*P < 0.05$, $^{\#}P < 0.05$, $^{\#\#}P < 0.05$.

siH19 or NC after 24 h culture with H_2O_2. Procedures for cells processing are shown in the Supplementary Materials (Fig. S1). Within 48 h of transfection, cell viability was decreased in the H/R and NC groups. However, viability in the H/R+NC and H/R+siH19 groups following 1 μM Dex postconditioning was significantly increased. Thus, Dex can regulate H19 expression in aged cardiomyocytes after H/R.

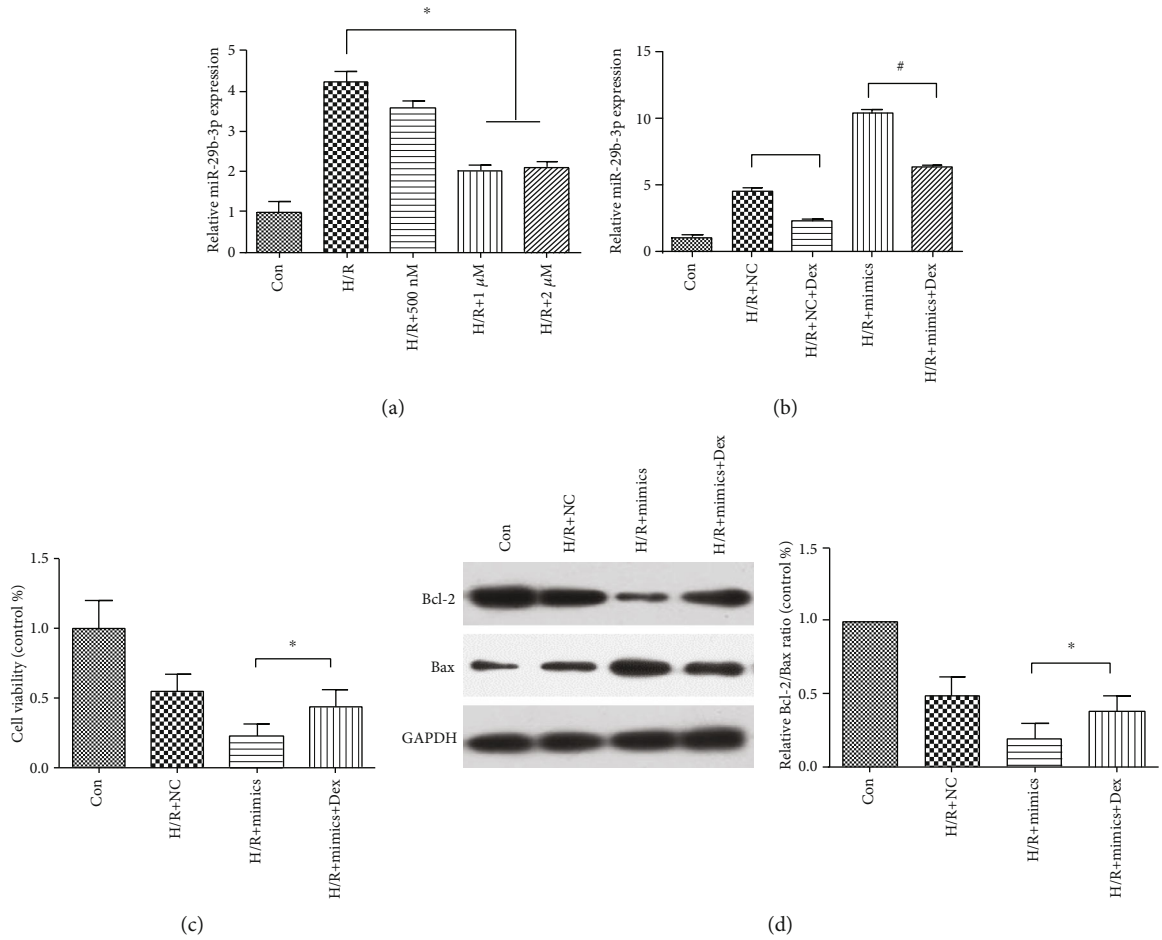

Figure 4: Protection of aging myocardial cells from hypoxia/reoxygenation (H/R) injury by dexmedetomidine (Dex) was enhanced by miR-29b-3p overexpression. Cell apoptosis was evaluated by flow cytometry. (a) Expression of miR-29b-3p after exposure to different concentrations of Dex and hypoxia postconditioning was detected by RT-PCR (mean ± SD, $n = 3$; $*P < 0.05$ vs. the H/R group). (b) Expression of miR-29b-3p in senescent cardiomyocytes, which were subjected to H/R treatment within 48 h of transfection with miR-29b-3p mimics or NC, as well as 6 h Dex postconditioning. (c) Cell viability was evaluated using a CCK-8 assay. (d) Expression of Bcl-2 and Bax was evaluated by western blotting. Mean ± SD, $n = 3$; $*P < 0.05$, $^{\#}P < 0.05$.

When H19 was knocked down in aged H9c2 cells, cell viability decreased and apoptosis rates increased after H/R. However, compared with the siH19+H/R group, Dex postconditioning still reduced apoptosis rates and increased cell viability (Figures 3(c) and 3(d)). Therefore, Dex postconditioning not only regulated the expression of H19 in aged cardiomyocytes following H/R but also reduced the injury induced by H/R with low H19 expression.

3.4. Dex Postconditioning Attenuated H/R Injury by Mediating miR-29b-3p/cIAP1. Our previous study revealed that H19 regulates expression of miR-29b-3p, and cIAP1 expression is mediated by miR-29b-3p and H19. Moreover, Dex postconditioning of aged cardiomyocytes reduced the injury induced by H/R with low H19 expression. Thus, we hypothesized that Dex postconditioning maintains its protective effect even in the context of abnormal expression of miR-29b-3p and cIAP1 in the aged heart. Compared with the control group, miR-29b-3p expression was increased after H/R, while its expression was decreased after 1 μM or 2 μM Dex postconditioning (Figure 4(a)). Furthermore, within 48 h of transfection with miR-29b-3p mimics, we observed decreased expression of miR-29b-3p in senescent cardiomyocytes subjected to H/R+Dex treatment compared with the H/R group (Figure 4(b)). Cell viability was increased with Dex postconditioning after overexpression of miR-29b-3p following 6 h hypoxia (Figure 4(c)). Compared with the H/R+miR-29b-3p group, the ratio of Bcl-2/Bax was increased following 6 h hypoxia with Dex postconditioning+miR-29b-3p (Figure 4(d)). Expression of cIAP1 was increased with 500 nM or 1 μM Dex postconditioning compared with the H/R group (Figure 5(a)). Within 48 h of transfection with cIAP1 siRNA and 6 h hypoxia, expression of cIAP1 (Figure 5(b)), cell viability, and Bcl-2/Bax ratios was increased compared with the H/R+sicIAP1 group (Figures 5(c) and 5(d)).

3.5. Dex Postconditioning Decreased m^6A Methylation and Increased ALKBH5 Expression in Aged Cardiomyocytes. First, we detected the effect of H/R and Dex postconditioning on

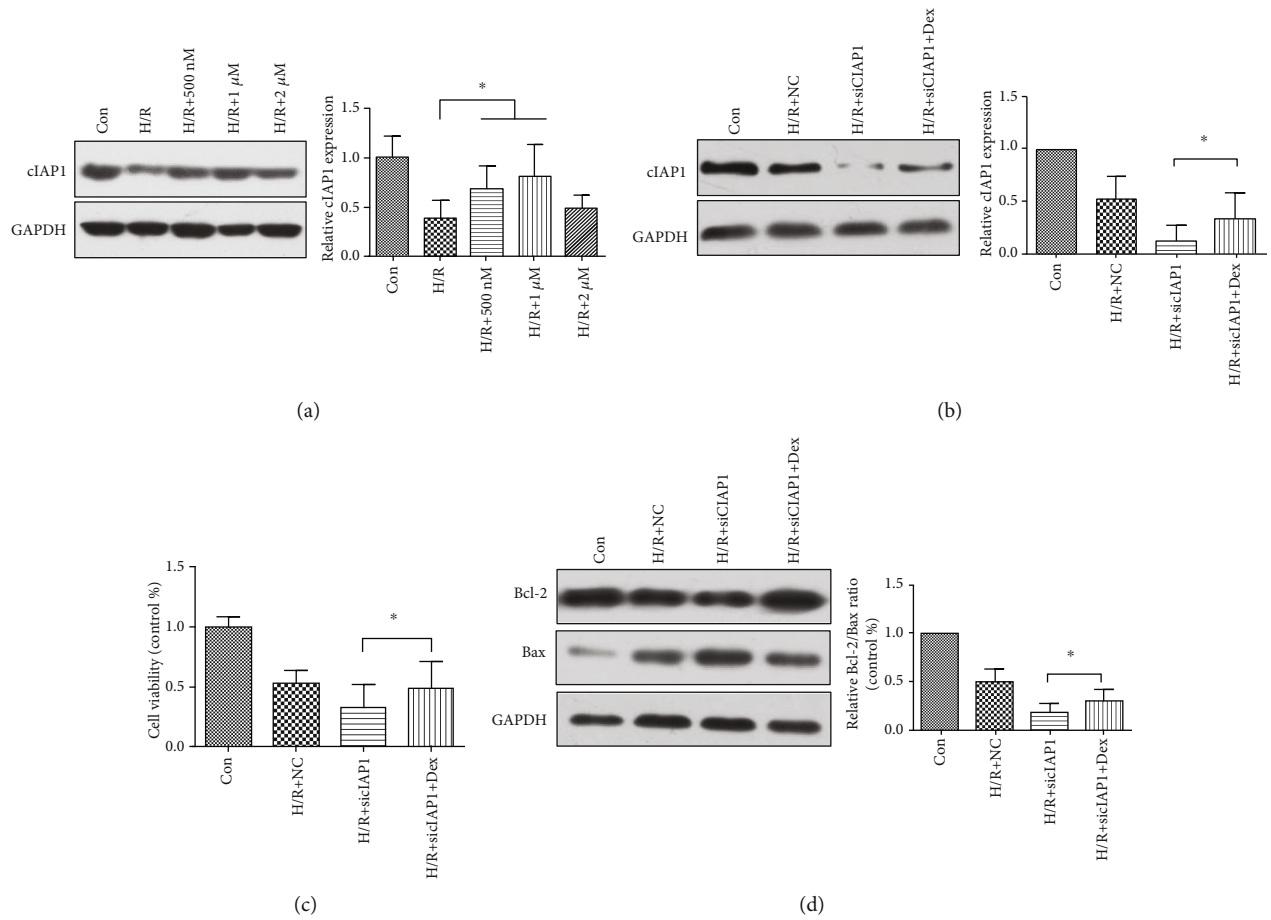

Figure 5: Attenuation of hypoxia/reoxygenation (H/R) injury by dexmedetomidine (Dex) postconditioning was enhanced by downregulation of cIAP1. (a) Western blotting was used to detect expression of cIAP1 after H/R and Dex postconditioning (mean ± SD, $n = 3$; $*P < 0.05$ vs. the H/R group). (b) Forty-eight hours after sicIAP1 or its control was transfected into senescent cardiomyocytes, cIAP1 expression levels were examined by western blot in cells exposed to 6 h hypoxia followed by 6 h Dex postconditioning or reoxygenation. (c, d) Effect of Dex in senescent cardiomyocytes subjected to H/R or altered expression of cIAP1. (c) Cell viability was evaluated using a CCK-8 assay. (d) Bcl-2 and Bax expression was evaluated by western blotting. Mean ± SD, $n = 3$; $*P < 0.05$.

m^6A modification. We observed that levels of m^6A modification increased after exposure to H/R but were decreased following Dex postconditioning in aged H9c2 cells (Figure 6(a)). Next, expression of m^6A modification-associated genes was measured by qRT-PCR. ALKBH5 was remarkably decreased after H/R at the mRNA level (Figure 6(b)). Finally, expression of ALKBH5 mRNA and protein levels after exposure to H/R and Dex postconditioning were detected. Compared with the H/R group, ALKBH5 expression was decreased after Dex postconditioning (Figures 6(c) and 6(d)).

3.6. ALKBH5 Regulated m^6A Modification of H19. As described above, H19 was decreased after H/R and increased after Dex postconditioning. ALKBH5 expression has a similar trend. Thus, we hypothesized that ALKBH5 and H19 have a regulatory relationship. We transfected siRNA to downregulate ALKBH5 expression (Figure 7(a)). After 48 h, H19 expression was decreased (Figure 7(b)). H9c2 cells were transfected with a vector encoding ALKBH5 or empty vector. ALKBH5 protein expression was detected after 48 h by western blot analysis (Figure 7(c)). When ALKBH5 was overexpressed, H19 expression was decreased (Figure 7(d)). However, with knockdown of H19 (Figure 7(e)), expression of ALKBH5 was not significantly altered at either mRNA or protein levels (Figures 7(f) and 7(g)). To investigate the mechanism by which ALKBH5 regulates H19, we knocked down ALKBH5 and measured m^6A methylation levels of H19. From our results, H19 m^6A methylation is increased after ALKBH5 knockdown in H9c2 cells (Figure 7(h)).

3.7. Dex Postconditioning Protected Aged H9c2 cells from H/R Injury Aggravated by ALKBH5 Knockdown. H9c2 cells were pretreated with H_2O_2 for 4 h, followed by transfection with siALKBH5 or its NC 24 h later. After 48 h of transfection, cells were exposed to hypoxia for 6 h, followed by reoxygenation or Dex postconditioning for 6 h. A CCK-8 assay was used to detect cell viability (Figure 8(a)), while flow cytometry and western blotting were used to measure apoptosis (Figures 8(b) and 8(c)). From the results, cell viability was decreased and proportions of apoptotic cells were increased with knockdown of ALKBH5 following H/R. However, Dex postconditioning protected aged H9c2 cells from H/R injury induced by downregulation of ALKBH5.

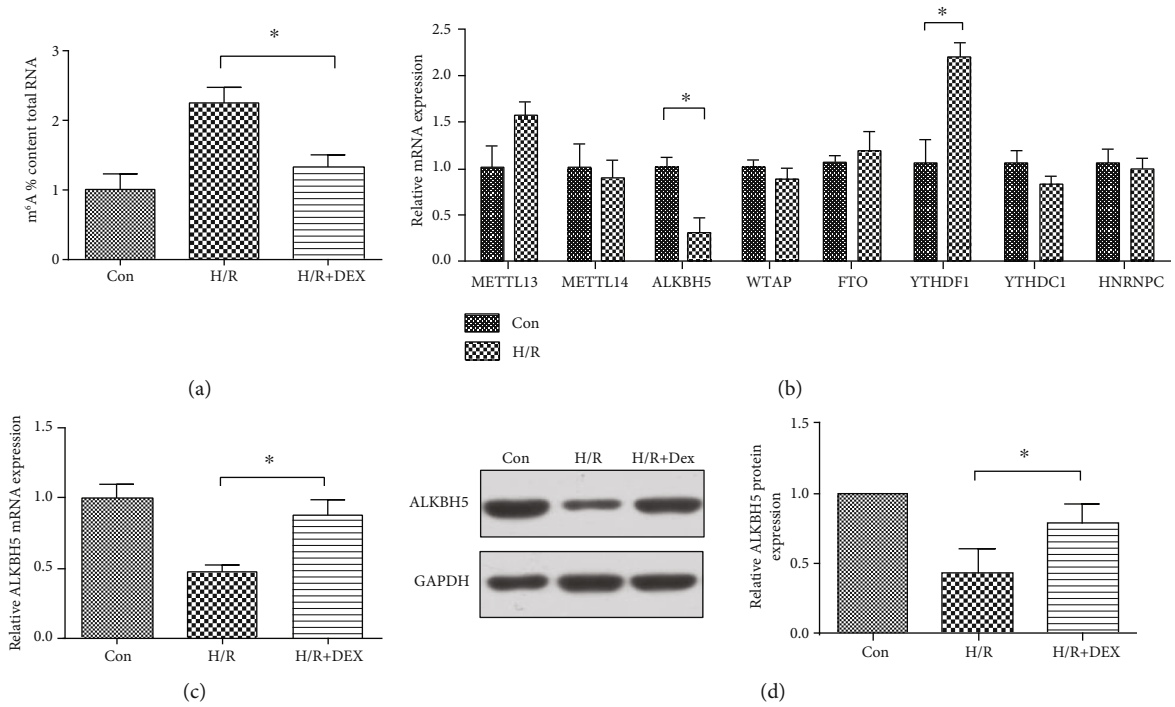

Figure 6: Dex postconditioning attenuated hypoxia/reoxygenation- (H/R-) induced increases of m^6A levels and downregulated ALKBH5 in aged H9c2 cells. (a) Colorimetry was used to detect total m^6A modification levels of RNA in aged myocardial cells after H/R and Dex postconditioning (mean ± SD, $n = 3$, $*P = 0.0014$). (b) mRNA levels of m^6A modification-associated genes were measured by qRT-PCR (mean ± SD, $n = 3$, $*P < 0.05$). (c) mRNA levels of ALKBH5 following H/R and H/R+Dex (mean ± SD, $n = 3$, $*P = 0.0037$). (d) ALKBH5 expression of cells exposed to H/R and H/R+Dex was measured by western blot (mean ± SD, $n = 3$, $*P = 0.0472$). Abbreviation: METTL3: methyltransferase like 3; METTL14: methyltransferase like 14; ALKBH5: alkB homolog 5; WTAP: Wilms tumor 1-associated protein; FTO: fat mass and obesity-associated protein; YTHDF1: YT521-B homology m6A-binding protein 1; YTHDC1: YT521-B homology domain-containing 1; HNRNPC: heterogeneous nuclear ribonucleoprotein C.

4. Discussion

According to our results, Dex postconditioning of aged myocardial cells reduced H/R-induced injury. H19 expression was decreased following H/R, while Dex hypoxic postconditioning increased H19 expression. Our previous study found that H19 regulated the expression of miR-29b-3p, and cIAP1 was mediated by miR-29b-3p and H19. In this study, Dex postconditioning reduced H/R-induced injury of aged cardiomyocytes via H19/miR-29b-3p/cIAP1. Moreover, levels of m^6A modification increased upon exposure to H/R but were decreased following Dex postconditioning in aged H9c2 cells. In addition, Dex postconditioning alleviated H/R injury induced by decreased ALKBH5 expression, and ALKBH5 regulated the expression of H19 by mediating its m^6A modification levels. Therefore, Dex plays a protective role against H/R-induced injury of aged myocardial cells through ALKBH5/H19/miR-29b-3p/cIAP1 (Figure 8(d)).

Ischemic disease is the leading cause of mortality worldwide, making identification of novel drug targets for protection of vital importance. In recent years, some studies found that Dex plays an important role in organ protection by regulating noncoding RNA. The neuroprotective effect of Dex on hippocampal neuronal cells in vitro was associated with miR-223-3p/TIAL1 [21]. Knockdown of the lncRNA MEG3 enhanced the protective effect of Dex against hypoxia-ischemia neonatal brain injury in mice [22]. Dex also attenuated lipopolysaccharide-induced acute lung injury via miR-381 [23]. Previous mechanistic studies of altered lncRNA expression in ischemic heart disease mainly focused on ceRNA as a regulator of microRNA expression [24, 25]. In addition, accumulating evidence proves the applicability of microRNAs as diagnostic biomarkers in ischemic heart disease [26]. The role of microRNAs in I/R injury has also been widely studied by altering the expression, and the hallmark of microRNA function is their ability to suppress gene expression by binding their target RNAs in a sequence-specific manner [27, 28]. According to our results, Dex reduced oxidative stress injury and apoptosis and increased cell viability of senescent cardiomyocytes after H/R. Moreover, we observed decreased H19 expression after H/R, but Dex postconditioning could increase H19 expression, even in the case of H19 knockdown. Dex also alleviated H/R-induced injury of aged cardiomyocytes, which was aggravated by the decline of H19 expression. In addition, our results indicated that Dex postconditioning alleviated H/R-induced injury of senescent myocardial cells by regulating miR-29b-3p/cIAP1.

As H19 was differentially expressed in the H/R and H/R +Dex postconditioning groups, we explored the upstream factors of H19. lncRNA could be regulated by epigenetic

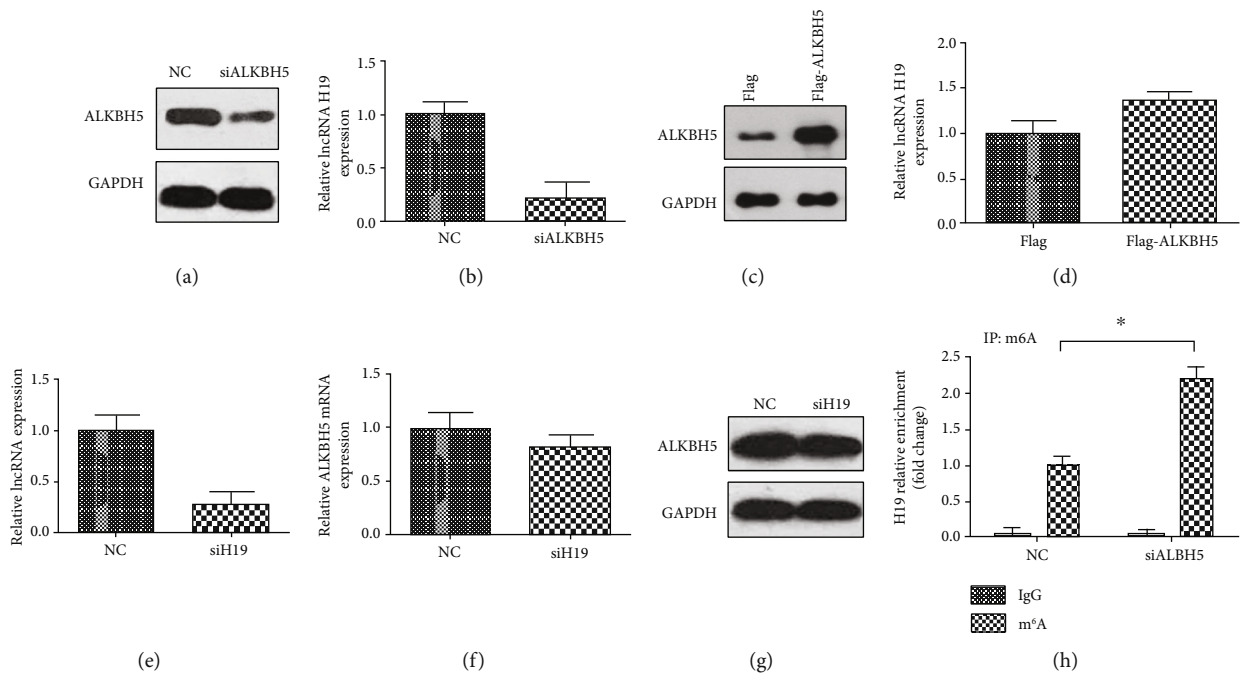

Figure 7: H19 undergoes m^{6}A modification via regulation of ALKBH5. (a) ALKBH5 protein expression was detected 48 h after knockdown by siRNA transfection using western blots. (b) Expression of H19 after transfection of siALKBH5 or NC was detected by qRT-PCR (mean ± SD, $n = 3$, $*P = 0.018$). (c) ALKBH5 protein expression was measured by western blot after transfection with a vector containing ALKBH5 or empty vector. (d) H19 expression after transfection with a vector encoding ALKBH5 or empty vector was detected by qRT-PCR (mean ± SD, $n = 3$, $P = 0.259$). (e) H9c2 cells were treated by transfection of siH19 to reduce expression of H19. The efficiency of transfection was detected by qRT-PCR after 48 h (mean ± SD, $n = 3$, $*P = 0.012$). (f) ALKBH5 mRNAs were detected by qRT-PCR (mean ± SD, $n = 3$, $P = 0.136$). (g) Protein expression levels of ALKBH5 were measured by western blot. (h) H19 m^{6}A methylation levels were measured after ALKBH5 knockdown (mean ± SD, $n = 3$, $*P < 0.001$).

modifications similar to coding genes and transcription factors [29]. 5′-Aza-2′-deoxycytidine, a compound that inhibits DNA methylation, and knockdown of DNA methyltransferase 1 restored H19 expression in hepatic stellate cells [30]. HIF-1α mediates lincRNA-p21 expression and plays an important role in the Warburg effect [31]. RNA m^{6}A methylation is the most abundant modification in both mRNA and lncRNA [32, 33]. The RNA m^{6}A demethylase ALKBH5 inhibited migration of pancreatic cancer cells by reducing methylation levels of the lncRNA KCNK15-AS1 [34]. Moreover, ALKBH5 regulates m^{6}A demethylation of NANOG mRNA to induce a breast cancer stem cell phenotype following hypoxia [35]. In our study, levels of m^{6}A modification increased after exposure to H/R but were decreased following Dex postconditioning in aged H9c2 cells. In addition, mRNA expression of ALKBH5 was remarkably decreased after H/R, as measured by qRT-PCR. However, YTHDF1 expression was significantly increased, but it was eliminated from analysis because of a large Ct value (mean ± SD, $n = 3$; con = 30.30 ± 0.12, H/R = 29.32 ± 0.08), most likely indicating a relatively low expression level (Figure 6(b)). Moreover, YTHDF1 promotes the rate-limiting step of translation for m^{6}A-modified mRNAs. After knockdown of YTHDF1, the m^{6}A-modified mRNAs were less associated with polysome [36]. Thus, we speculated that it has relatively lower effect on the expression of noncoding RNA. Therefore, ALKBH5 was the focus of our research and we found that ALKBH5 regulates H19 expression by mediating its level of m^{6}A methylation. Knockdown of ALKBH5 aggravated H/R injury but was attenuated by 1 μM Dex postconditioning.

In the future, we aim to examine the expression of ALKBH5 and its downstream genes, as well as evaluate myocardial protective effects of ALKBH5 and Dex following I/R *in vivo*. Moreover, we plan to explore the mechanism by which ALKBH5 regulates H19 expression, as it is possible that m^{6}A affects the stability of H19, but the mechanism remains to be fully elucidated. Despite the fact much work remains to be done to translate cardioprotective therapies from the research laboratory into the clinical settings to improve prognosis in patients, the discovery of a novel cardioprotective effect and mechanism of Dex hypoxia postconditioning will provide the new strategies for the prevention of I/R injury in elderly patients.

5. Conclusions

The levels of total RNA m^{6}A modification increased after exposure to H/R but were decreased following Dex postconditioning in aged H9c2 cells. In addition, ALKBH5 expression was decreased after Dex postconditioning and ALKBH5 mediated H19 expression by regulating its level of m^{6}A methylation. Finally, Dex postconditioning protected against H/R injury in aged H9c2 cells by regulating the expressions of ALKBH5/H19/miR-29b-3p/cIAP1. As Dex is

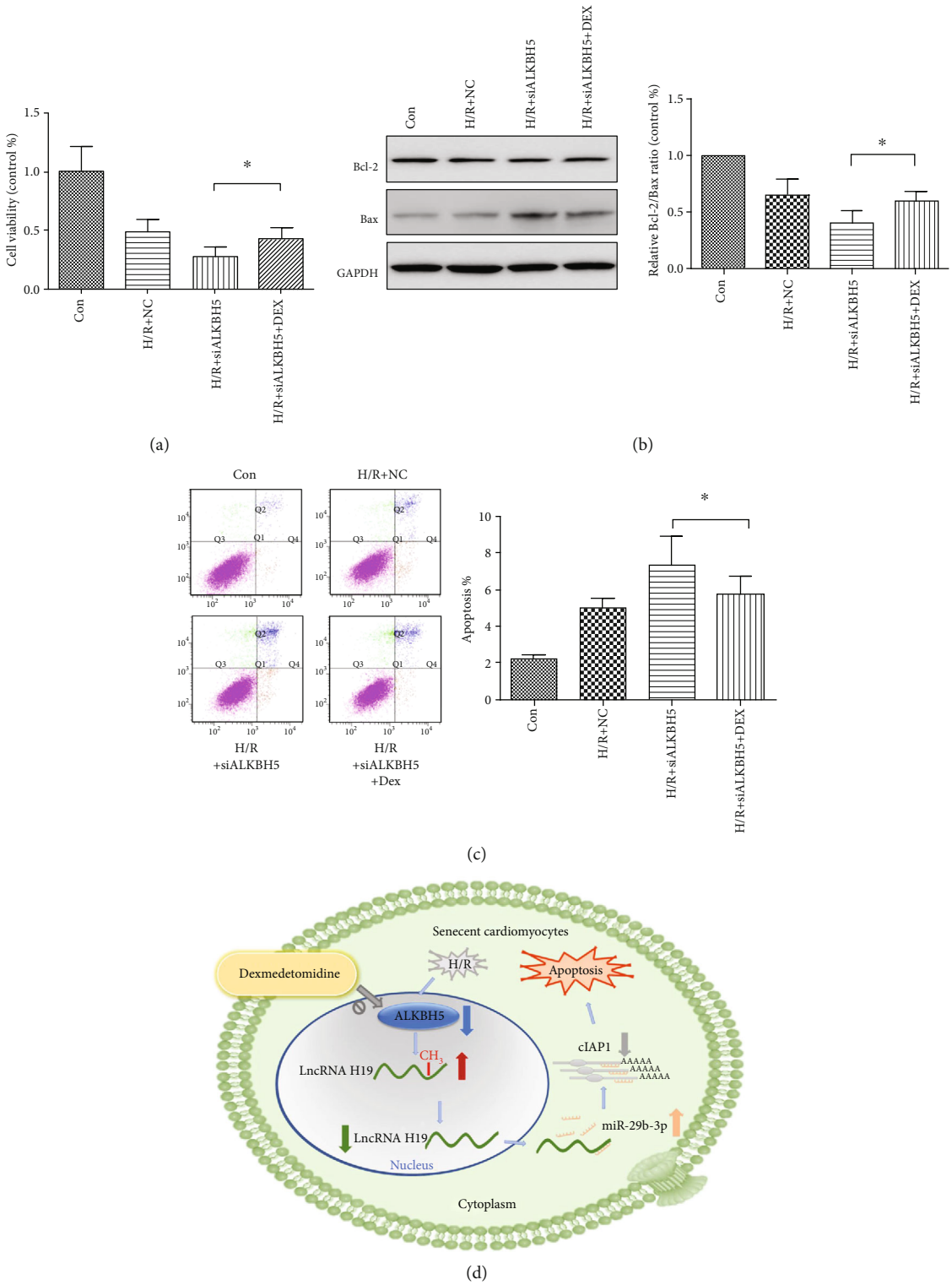

Figure 8: Dex postconditioning protected aged H9c2 cells from aggravation of hypoxia/reperfusion (H/R) injury by ALKBH5 knockdown. H9c2 cells pretreated with H_2O_2 for 4 h were transfected with siALKBH5 or its NC 24 h later. Within 48 h of transfection, aged H9c2 cells were exposed to hypoxia for 6 h and either reoxygenation or Dex postconditioning for 6 h. (a) A CCK-8 assay was used to detect cell viability. (b) Flow cytometry was used to measure proportions of apoptotic cells. (c) Western blotting was used to evaluate protein expression of Bcl-2 and Bax. Mean ± SD, $n = 3$, $*P < 0.05$. (d) Schematic showing mechanisms of action for Dex in aged cardiomyocytes following H/R. ALKBH5 expression was decreased following H/R in senescence cardiomyocytes but thus was attenuated by Dex postconditioning. m^6A methylation levels and H19 expression were regulated by ALKBH5. H19 expression was decreased following H/R. Subsequently, isolated miR-29b-3p increased binding to the $3'$-UTR region of cIAP1 and decreased its expression, leading to increased apoptosis.

commonly used as an intravenous anesthetic during the perioperative period not the drugs routinely implemented after MI, therefore the cardioprotective mechanism of Dex hypoxia postconditioning explored in our research has clinical relevance for identifying valid drug targets and precise therapeutic approaches for aged MI patients.

Data Availability

The data used to support the findings of this study are available from the corresponding authors upon request.

Conflicts of Interest

The authors declare that they have no competing interests.

Acknowledgments

This research was conducted with the support of the National Key R&D Plan of China (No. 2018YFC2001900), National Natural Science Foundation of China (81601209), and Beijing Novo Program (No. Z181100006218073).

Supplementary Materials

Supplemental Table 1: list of abbreviations. Supplemental Table 2: primers used for real-time PCR and siRNA sequences. Figure S1: experimental groupings and protocols. H_2O_2 was added into DMEM for 4 h to induce the senescence of H9c2 cells. After 24 h, cells were transfected with NC or siRNA/mimics. The medium of the H/R group was changed to HBSS, and cells were kept in an incubator for 6 h of hypoxia. The H/R and control groups were replaced with DMEM containing FBS, while Dex postconditioning groups were treated with different concentrations of Dex during 6 h reoxygenation. *(Supplementary Materials)*

References

[1] P. Ferdinandy, R. Schulz, and G. F. Baxter, "Interaction of cardiovascular risk factors with myocardial ischemia/reperfusion injury, preconditioning, and postconditioning," *Pharmacological Reviews*, vol. 59, no. 4, pp. 418–458, 2007.

[2] H. J. Priebe, "The aged cardiovascular risk patient," *British Journal of Anaesthesia*, vol. 85, no. 5, pp. 763–778, 2000.

[3] I. Y. Choi, L. Hwang, J. J. Jin et al., "Dexmedetomidine alleviates cerebral ischemia-induced short-term memory impairment by inhibiting the expression of apoptosis-related molecules in the hippocampus of gerbils," *Experimental and Therapeutic Medicine*, vol. 13, no. 1, pp. 107–116, 2017.

[4] J. M. Gao, X. W. Meng, J. Zhang et al., "Dexmedetomidine Protects Cardiomyocytes against Hypoxia/Reoxygenation Injury by Suppressing TLR4-MyD88-NF- κ B Signaling," *Biomed Research International*, vol. 2017, Article ID 1674613, 13 pages, 2017.

[5] M. Zhai, C. Liu, Y. Li et al., "Dexmedetomidine inhibits neuronal apoptosis by inducing Sigma-1 receptor signaling in cerebral ischemia-reperfusion injury," *Aging*, vol. 11, no. 21, pp. 9556–9568, 2019.

[6] Y. Wang, S. Wu, X. Yu et al., "Dexmedetomidine protects rat liver against ischemia-reperfusion injury partly by the α2A-adrenoceptor subtype and the mechanism is associated with the TLR4/NF-κB pathway," *International Journal of Molecular Sciences*, vol. 17, no. 7, p. 995, 2016.

[7] F. Ji, Z. Li, H. Nguyen et al., "Perioperative dexmedetomidine improves outcomes of cardiac surgery," *Circulation*, vol. 127, no. 15, pp. 1576–1584, 2013.

[8] X. Y. Cheng, X. Gu, Q. Gao, Q. Zong, X. Li, and Y. Zhang, "Effects of dexmedetomidine postconditioning on myocardial ischemia and the role of the PI3K/Akt-dependent signaling pathway in reperfusion injury," *Molecular Medicine Reports*, vol. 14, no. 1, pp. 797–803, 2016.

[9] S. Lecour, H. E. Bøtker, G. Condorelli et al., "ESC working group cellular biology of the heart: position paper: improving the preclinical assessment of novel cardioprotective therapies," *Cardiovascular Research*, vol. 104, no. 3, pp. 399–411, 2014.

[10] L. Salmena, L. Poliseno, Y. Tay, L. Kats, and P. P. Pandolfi, "A ceRNA hypothesis: the Rosetta Stone of a hidden RNA language?," *Cell*, vol. 146, no. 3, pp. 353–358, 2011.

[11] W. P. Tsang, E. K. O. Ng, S. S. M. Ng et al., "Oncofetal H19-derived miR-675 regulates tumor suppressor RB in human colorectal cancer," *Carcinogenesis*, vol. 31, no. 3, pp. 350–358, 2010.

[12] X. Li, S. Luo, J. Zhang et al., "lncRNA H19 alleviated myocardial I/RI via suppressing miR-877-3p/Bcl-2-mediated mitochondrial apoptosis," *Molecular Therapy - Nucleic Acids*, vol. 17, pp. 297–309, 2019.

[13] T. Yoshimizu, A. Miroglio, M. A. Ripoche et al., "The H19 locus acts in vivo as a tumor suppressor," *Proceedings of the National Academy of Sciences of the United States of America*, vol. 105, no. 34, pp. 12417–12422, 2008.

[14] Z. Xiao, Y. Qiu, Y. Lin et al., "Blocking lncRNA *H19*-miR-19a-Id2 axis attenuates hypoxia/ischemia induced neuronal injury," *Aging*, vol. 11, no. 11, pp. 3585–3600, 2019.

[15] J. Wang, H. Zhao, Z. Fan et al., "Long noncoding RNA H19 promotes neuroinflammation in ischemic stroke by driving histone deacetylase 1-dependent M1 microglial polarization," *Stroke*, vol. 48, no. 8, pp. 2211–2221, 2017.

[16] L. C. Gong, H. M. Xu, G. L. Guo, T. Zhang, J. W. Shi, and C. Chang, "Long non-coding RNA H19 protects H9c2 cells against hypoxia-induced injury by targeting MicroRNA-139," *Cellular Physiology and Biochemistry*, vol. 44, no. 3, pp. 857–869, 2017.

[17] X. Zhang, L. Cheng, L. Xu et al., "The LncRNA, H19 mediates the protective effect of hypoxia postconditioning against hypoxia-reoxygenation injury to senescent cardiomyocytes by targeting microRNA-29b-3p," *Shock*, vol. 52, no. 2, pp. 249–256, 2019.

[18] J. Tong, R. A. Flavell, and H. B. Li, "RNA m^6A modification and its function in diseases," *Frontiers of Medicine*, vol. 12, no. 4, pp. 481–489, 2018.

[19] H. Song, X. Feng, H. Zhang et al., "METTL3 and ALKBH5 oppositely regulate m^6A modification of *TFEB* mRNA, which dictates the fate of hypoxia/reoxygenation-treated cardiomyocytes," *Autophagy*, vol. 15, no. 8, pp. 1419–1437, 2019.

[20] D. Dominissini, S. Moshitch-Moshkovitz, M. Salmon-Divon, N. Amariglio, and G. Rechavi, "Transcriptome-wide mapping of N(6)-methyladenosine by m(6)A-seq based on immunocapturing and massively parallel sequencing," *Nature Protocols*, vol. 8, no. 1, pp. 176–189, 2013.

[21] Q. Wang, H. Yu, H. Yu, M. Ma, Y. Ma, and R. Li, "miR-223-3p/TIAL1 interaction is involved in the mechanisms

associated with the neuroprotective effects of dexmedetomidine on hippocampal neuronal cells in vitro," *Molecular Medicine Reports*, vol. 19, no. 2, pp. 805–812, 2019.

[22] X. M. Zhou, J. Liu, Y. Wang, and M. H. Zhang, "Silencing of long noncoding RNA MEG3 enhances cerebral protection of dexmedetomidine against hypoxic-ischemic brain damage in neonatal mice by binding to miR-129-5p," *Journal of Cellular Biochemistry*, vol. 120, no. 5, pp. 7978–7988, 2018.

[23] Y. Zhang, X. Wang, Z. Liu, and L. Yu, "Dexmedetomidine attenuates lipopolysaccharide induced acute lung injury by targeting NLRP3 via miR-381," *Journal of Biochemical and Molecular Toxicology*, vol. 32, no. 11, p. e22211, 2018.

[24] H. Zhai, X. M. Li, F. Liu et al., "Expression pattern of genome-scale long noncoding RNA following acute myocardial infarction in Chinese Uyghur patients," *Oncotarget*, vol. 8, no. 19, pp. 31449–31464, 2017.

[25] K. Wang, C. Y. Liu, L. Y. Zhou et al., "APF lncRNA regulates autophagy and myocardial infarction by targeting miR-188-3p," *Nature Communications*, vol. 6, no. 1, 2015.

[26] Z. Varga, Z. Giricz, P. Bencsik et al., "Functional genomics of cardioprotection by ischemic conditioning and the influence of comorbid conditions: implications in target identification," *Current Drug Targets*, vol. 16, no. 8, pp. 904–911, 2015.

[27] Y. Shen, Z. Shen, L. Miao et al., "miRNA-30 family inhibition protects against cardiac ischemic injury by regulating cystathionine-γ-lyase expression," *Antioxidants & Redox Signaling*, vol. 22, no. 3, pp. 224–240, 2015.

[28] N. Yang, L. Wu, Y. Zhao, N. Zou, and C. Liu, "MicroRNA-320 involves in the cardioprotective effect of insulin against myocardial ischemia by targeting survivin," *Cell Biochemistry and Function*, vol. 36, no. 3, pp. 166–171, 2018.

[29] N. Liu, M. Parisien, Q. Dai, G. Zheng, C. He, and T. Pan, "Probing N6-methyladenosine RNA modification status at single nucleotide resolution in mRNA and long noncoding RNA," *RNA*, vol. 19, no. 12, pp. 1848–1856, 2013.

[30] J. J. Yang, Q. She, Y. Yang, H. Tao, and J. Li, "DNMT1 controls LncRNA H19/ERK signal pathway in hepatic stellate cell activation and fibrosis," *Toxicology Letters*, vol. 295, pp. 325–334, 2018.

[31] F. Yang, H. Zhang, Y. Mei, and M. Wu, "Reciprocal regulation of HIF-1α and lincRNA-p 21 modulates the Warburg effect," *Molecular Cell*, vol. 53, no. 1, pp. 88–100, 2014.

[32] D. Dominissini, S. Moshitch-Moshkovitz, S. Schwartz et al., "Topology of the human and mouse m^6A RNA methylomes revealed by m^6A-seq," *Nature*, vol. 485, no. 7397, pp. 201–206, 2012.

[33] I. A. Roundtree, M. E. Evans, T. Pan, and C. He, "Dynamic RNA modifications in gene expression regulation," *Cell*, vol. 169, no. 7, pp. 1187–1200, 2017.

[34] Y. He, H. Hu, Y. Wang et al., "ALKBH5 inhibits pancreatic cancer motility by decreasing long non-coding RNA KCNK15-AS1 methylation," *Cellular Physiology and Biochemistry*, vol. 48, no. 2, pp. 838–846, 2018.

[35] C. Zhang, D. Samanta, H. Lu et al., "Hypoxia induces the breast cancer stem cell phenotype by HIF-dependent and ALKBH5-mediated m^6A-demethylation of NANOG mRNA," *Proceedings of the National Academy of Sciences*, vol. 113, no. 14, pp. E2047–E2056, 2016.

[36] X. Wang, B. S. Zhao, I. A. Roundtree et al., "N^6-methyladenosine Modulates Messenger RNA Translation Efficiency," *Cell*, vol. 161, no. 6, pp. 1388–1399, 2015.